Geometry, number theory, and the butterfly spectrum of two-dimensional Bloch electrons

Indubala I. Satija ⬤

Department of Physics and Astronomy, George Mason University, Fairfax, Virginia 22030, USA

We take a deeper dive into the geometry and the number theory that underlay the butterfly graphs of the Harper and the generalized Harper models of Bloch electrons in a magnetic field. The root of the number theoretical characteristics of the fractal spectrum is traced to a close relationship between the Farey tree—the hierarchical tree that generates all rationals and the Wannier diagram—a graph that labels all the gaps of the butterfly graph. The resulting Farey-Wannier hierarchical lattice of trapezoids provides a geometrical representation of the nested pattern of butterflies in the butterfly graph. Some features of the energy spectrum, such as absence of some of the Wannier trajectories in the butterfly graph falling outside the number theoretical framework, can be stated as a simple rule of minimal violation of mirror symmetry. In a generalized Harper model, number theoretical framework prevails with the Farey-Wannier hierarchical lattice regrouping to form some hexagonal cells creating different *species* of butterflies.

I. INTRODUCTION

The butterfly graph—a quantum fractal, is a graph of energy spectrum of Bloch electrons in a two-dimensional square lattice subjected to a traverse magnetic field. Resembling a butterfly, it consists of self-similar pattern of nested sets of copies of itself. Commonly referred as the Hofstadter butterfly after its discovery by Douglas Hofstadter in 1976 [1], the subject has attracted a broad spectrum of physics and the mathematics community [2–4]. Furthermore, there have been various recent attempts to capture this iconic spectrum in various laboratories [5]. The butterfly graph as a whole describes all possible phases, the integer quantum Hall states, of a two-dimensional electron gas [6] that arise as one varies the electron density and the magnetic field. Each phase is characterized by an integer that represents the quantum number of Hall conductivity. Recent studies [2,7–9] have described various features of the butterfly spectrum using pure number theoretical reasoning and the quantum fractal is found closely related to some abstract mathematical sets.

In this paper, we further examine the role of the number theory in this quantum system where competition between a crystalline lattice and cyclotron radius lies at the very heart of the emergent hierarchical spectrum. We show that the Farey tree—a hierarchical set that generates all prime fractions between zero and one and the Wannier diagram, which provides a simple representation of the butterfly graph, are closely related. Figure 1 highlights the number theoretical aspect of the butterfly graph—a fractal made up of integers where the integers represent the quantum numbers of Hall conductivity. They appear as the slopes of straight line trajectories in a unit square, the Wannier diagram. Furthermore, the nesting of the butterfly spectrum is encoded in the Farey tree hierarchy. Superposing the butterfly graph and the Wannier diagram as shown in the rightmost panel in Fig. 1 unveils a hierarchical

lattice of trapezoids dubbed a Farey-Wannier lattice, where every butterfly in the butterfly graph can be paired with a trapezoid in the lattice. Our observation that the lattice excludes certain trapezoidal configurations that do not represent butterfly patterns, falls outside number theoretical framework. Such patterns are found to be described by a simple rule where the forbidden configurations correspond to "higher order" violation of the symmetries of the butterflies.

In addition to the Harper model [10], the nearest-neighbor (NN) tight-binding model of two-dimensional Bloch electrons in magnetic field, we also discuss a generalized next-nearest-neighbor (NNN) model [11–15] and show that Farey hierarchy prevails in characterizing the hierarchical structure of the energy spectrum. In the latter case, the Farey-Wannier lattice regroups to form hexagonal cells that describe butterflies with somewhat different number theoretical characteristics. In our limited exploration, the butterfly recursions for the generalized Harper equation is found to be described by the scaling factors $\zeta = [n^* + 1; \overline{1, n^*}]$ that underlie the scalings of the the Harper equation spectrum. However, renormalization equations rooted in the Farey tree hierarchy leave open the possibility of universality classes that describe self-similar butterfly scalings in the generalized Harper model.

It is interesting and important to address the role of number theory in characterizing some features of the butterfly graph in various investigations of the variations of the Harper model—a subject that continues to fascinate the scientific community. In such studies, based mostly on numerics, number theoretical tools are a great asset, as shown the case of a recent study of perturbing the butterfly graph with density waves [16]. In this paper, the Wannier-like diagram was found to provide a useful insight toward the topological integers that label the gaps and characterize an unusual kind of quantum Hall effects in the system. This suggests the robustness of the role of number theory in determining the spectral characteristics of butterfly
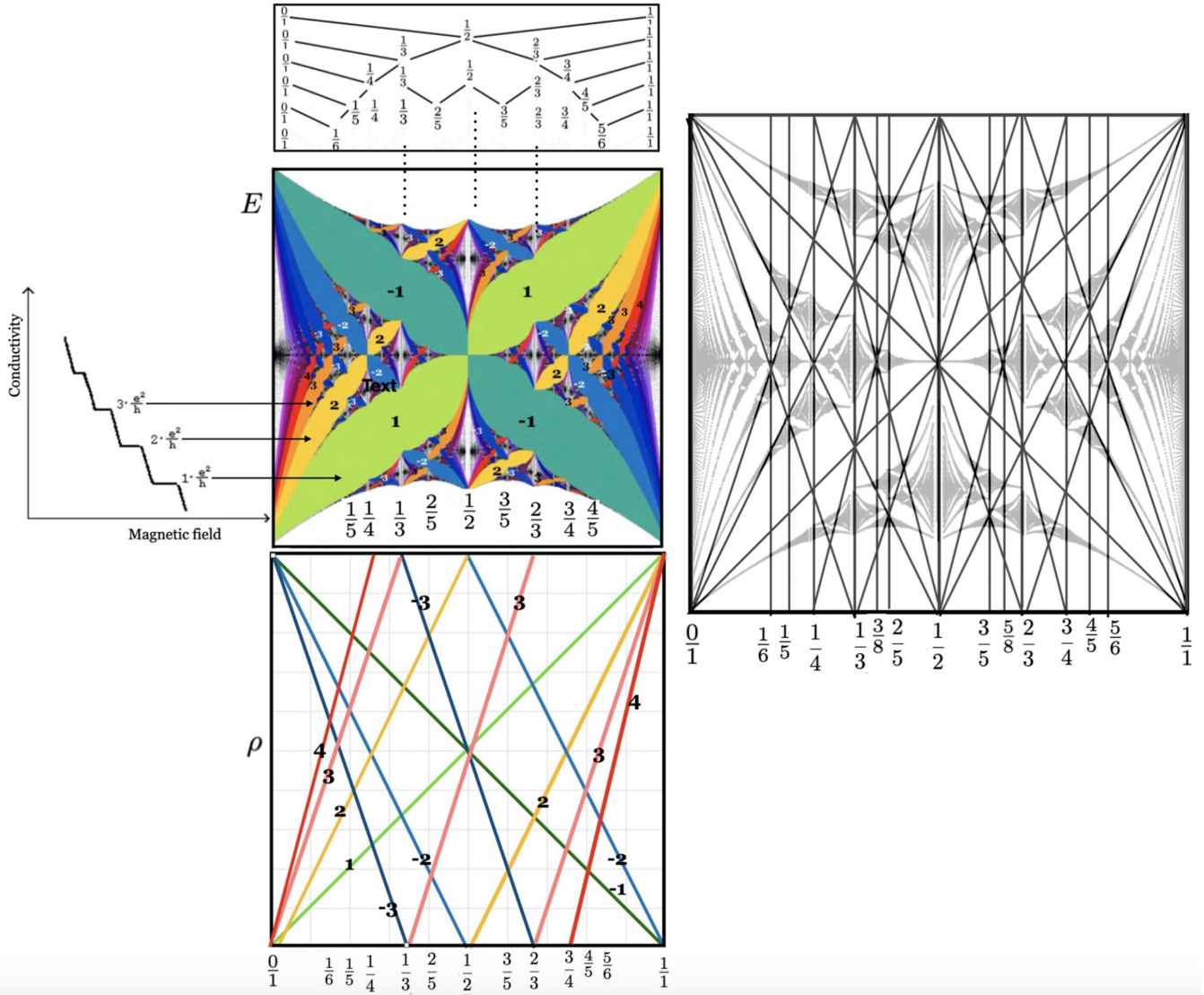
FIG. 1. Sketch of plateau of Hall conductivity (left) and the butterfly graph where gaps are labeled with quantum numbers of the Hall conductivity as shown by the arrows. The three vertical panels at the center portray the relationship between the butterfly graph (central panel) and abstract mathematical hierarchical sets—namely, the Farey tree (top panel) and the Wannier diagram (bottom panel). In the rightmost panel, the butterfly graph and the Wannier diagram are superimposed. This illustrates how the Wannier diagram provides a geometrical representation of the butterfly graph as the boundaries and the centers of the butterflies are encoded in the Wannier trajectories.

graphs for a wide class of systems with competing length scales.

In Sec. II, we began with a brief review of the butterfly Hamiltonian and its relation with the Farey tree and the Wannier diagram. Section III uses the mathematical framework described in an earlier study [17] to show that the Farey Free and the Wannier diagram are closely related. We would like to point out that the importance of the Farey tree and the Wannier diagram in the butterfly problem has been discussed extensively in the past. However, to best of our knowledge, the relationship between these two hierarchical sets has not been known or discussed before.

Section IV introduces a Farey-Wannier hierarchical lattice of trapezoids that provides insight toward its relation to the butterfly graph. In particular, every butterfly in the butterfly graph can be paired with a trapezoidal cell in the Wannier

diagram. However, the converse is not true. Based on very detailed numerical studies, we show that not all Wannier trajectories lead to the formation of butterflies. This empirical result that falls outside the number theoretical reasoning is found to be related to an observation that the allowed butterfly configurations correspond to minimum violation of geometrical mirror symmetry.

Section V discusses a generalized Harper model with unique species of butterflies. In the Appendix, we review earlier work [17] describing self-similar Farey hierarchy as a conformal map. The resulting Möbius transformation is identical to the self-similar butterfly recursion discussed recently [8,9]. The number theoretical origin of these recursions extend their applicability to describe self-similar hierarchies of the NNN model and therefore provides another perspective on hierarchical structures related to the Farey tree.

II. THE BUTTERFLY GRAPH

The butterfly Hamiltonian, the Harper model, is a simple model of two-dimensional noninteracting, spinless electrons in a perpendicular magnetic field B where electrons moving in a square lattice can hop only to its NN sites. The key parameter in the problem is the magnetic flux per unit cell of the lattice in the units of the flux quanta $\phi = \frac{Ba^2}{\hbar/e}$. In its simplest form, the model can be written as [18,19]

$$H = \cos x + \cos p, \quad [x, p] = i\phi, \quad (1)$$

that is, a butterfly graph lives in the space of energy E and the effective Planck's constant ϕ. The graph resembles a butterfly with a highly intricate recursive structure, consisting of nothing but copies of itself, the sub-butterflies, nested infinitely deeply.

For a rational flux $\phi = \frac{p}{q}$, the butterfly spectrum consists of q bands, separated by $(q - 1)$ gaps that form the wings of the butterfly. For q even, the two bands touch at the center of the spectrum, that is, at $E = 0$. For the irrational case, the spectrum is a Cantor set where the allowed values of the energy is set of zero measure. This is known as the ten martini problem—the name was coined by Barry Simon in his 1982 article [20], originating from the fact that Mark Kac offered ten martinis to anyone who solves it.

A. Identifying subimages as butterflies

In the butterfly graph, infinitely nested sub-butterflies that have lost most of the symmetries of the main butterfly may be difficult to identify. Below we state what images qualify as the "butterflies", which are also referred as sub-butterflies.

In a given magnetic flux interval with the left and right edges labeled as $\phi_L = \frac{p_L}{q_L}$ and $\phi_R = \frac{p_R}{q_R}$, a butterfly is identified when a single band at the left edge *reforms* again at the right edge. In between the two edges, the bands split, forming a very intricate fractal structure where, miraculously, the gaps between the bands form smooth channels. The four dominant gaps emanating from the four corners corresponding to the upper and lower edges of the two bands meet at a flux value labeled $\phi_c = \frac{p_c}{q_c}$, identified as the center of the butterfly. These features are very distinct in the main butterfly formed by single bands at $\phi = 0$ and $\phi = 1$ and center at $\phi_c = \frac{1}{2}$ but may be somewhat opaque in a very distorted region of the butterfly graph. As seen later, while discussing figures such as Figs. 8 and 9, this criterion provides an unambiguous way to identify sub-butterflies in the Harper as well as the generalized Harper model.

We note that in the Harper model, the sub-butterflies in the region between ϕ_L and ϕ_R are well- approximated by a distorted version of the original Hofstadter butterfly [8,18]. However, in a generalized NNN-Harper model, different species of butterflies appear which are not related to the main butterfly. In spite of not being the exact replica of the main butterfly, they can be identified as sub-butterflies without any doubt or uncertainty.
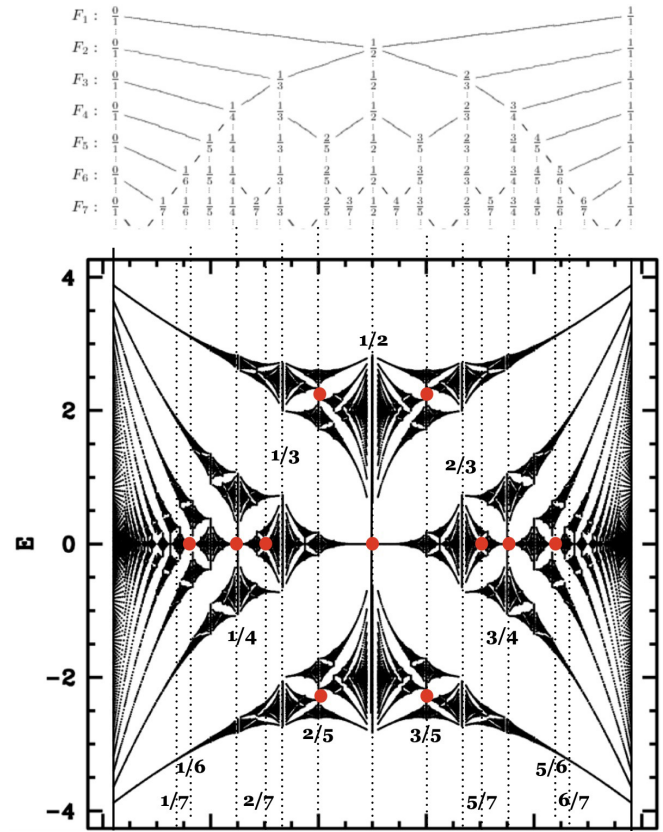

FIG. 2. The Farey Tree and the butterfly graph. The left-right boundaries and the center of every sub-butterfly in the graph can be labeled with a friendly Farey triplet.

B. Wannier diagram—butterfly skeleton

The Wannier diagram was named after Gregory Wannier, who in 1978 revisited [21,22] the problem of a crystal in a magnetic field shortly after the discovery of the butterfly graph. It provides a simple representation of the spectrum by labeling all the gaps of the spectrum with two integers (σ, τ), expressed as a linear Diophantine equation:

$$r = p\sigma + \tau q, \quad \rho \equiv \frac{r}{q} = \sigma\phi + \tau. \quad (2)$$

Here r labels the rth gap of the spectrum for a rational magnetic flux $\phi = \frac{p}{q}$ and ρ is the density of the electrons or the fraction of total number of states below Fermi energy. The ρ vs ϕ plot can be viewed as representing the butterfly skeleton as various Wannier trajectories representing the gaps of the butterfly shrink to straight lines. For a given set of values for (r, p, q), there are infinitely many solutions to any such Diophantine equation. Indeed, it is easy to see that if (σ, τ) is a solution of equation, then so is $(\sigma + nq, \tau - np)$, $n = 0, \pm 1, \pm 2 \ldots$. It turns out that for the rectangular lattice, what we want is the smallest possible σ (in absolute value).

In 1982, the linear Diophantine equation got a big boost after Thouless *et al.* [6] showed that the integer σ in Eqs. (2) represents the quantum number of Hall conductivity and has topological origin. Following this important discovery for which David Thouless was awarded the Nobel prize in (2016), Eqs. (2) has been the subject of various studies [12,23–26] and
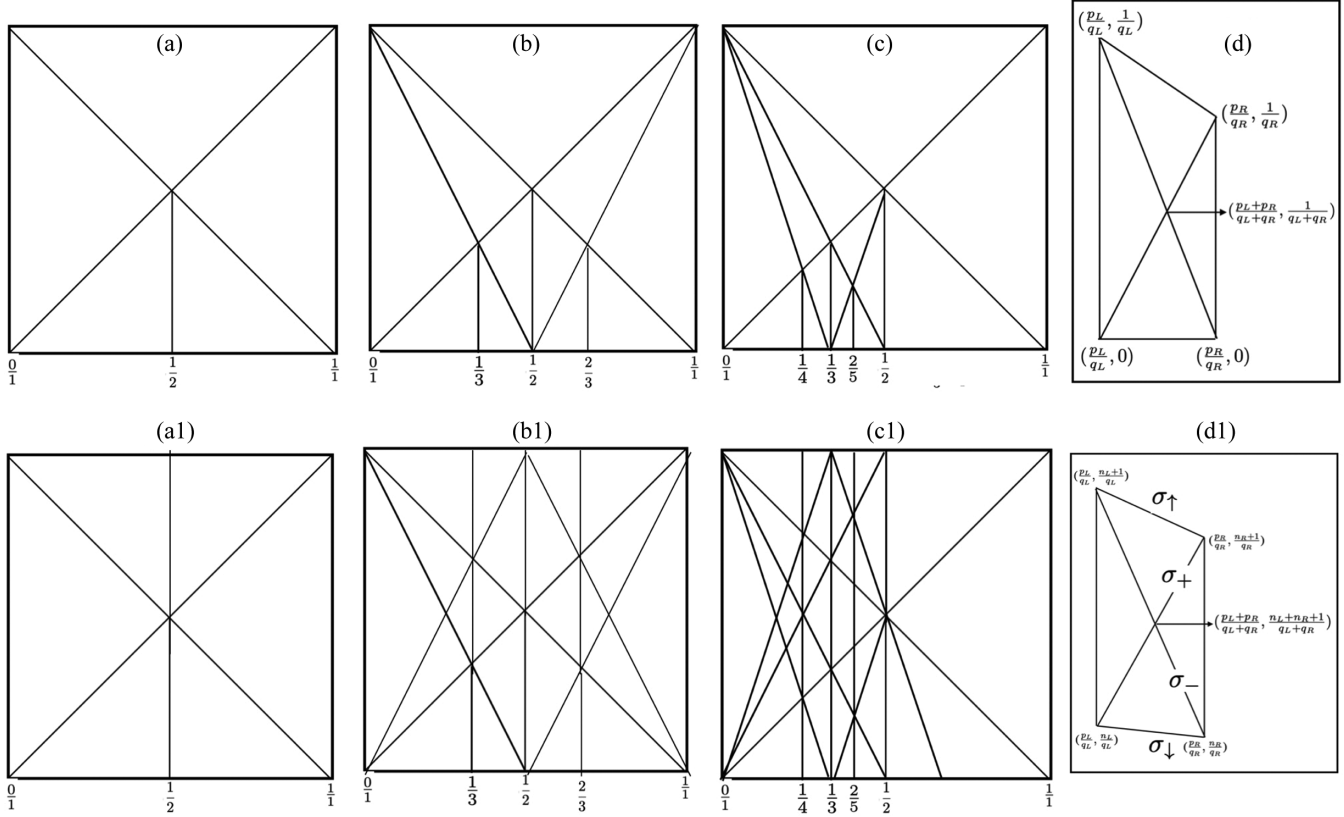
FIG. 3. (a)–(c) show an alternative way to construct the Farey tree using straight lines in a square. Lower panel:(a1)–(c1) show the corresponding Wannier diagram. Panels (d) and (d1), respectively, show a general trapezoid in the Farey and in the Wannier construction, with the coordinates of the four corners labeled. (d1) also labels the slopes of the nonparallel lines as $(\sigma_\uparrow, \sigma_\downarrow)$ and the slopes of the diagonals as (σ_+, σ_-).

is also referred to as the the gap labeling theorem [20]. In a recent experimental investigation of the butterfly spectrum [5], the calculation of (σ, τ) from the measurement of the filling-fraction ρ emerged as the key factor in providing laboratory glimpses of the butterfly fractal.

C. Farey tree and the butterfly graph

Although the connection between the butterfly graph and the Wannier diagram has been known since 1978, the relationship between the hierarchical nature of the butterfly graph and the Farey tree was pointed out in 2016 [2,7]. In 2020, these empirical results were derived [8] using a previously known renormalization group [18], thus establishing the fact that the quantum mechanics of the Bloch electrons in a magnetic field is intertwined with various number theoretical results. Below we briefly review the Farey tree construction and its relationship with the butterfly graph.

Discovered by Adolf Hurwitz in 1894, the Farey tree generates all primitive rationals between 0 and 1. As shown in Fig. 2, this hierarchical treelike structure builds the entire set of rationals by starting with 0 and 1. Given any two fractions $\frac{p_L}{q_L}$ and $\frac{p_R}{q_R}$ that satisfy

$$p_L q_R - p_R q_L = \pm 1, \qquad (3)$$

then p_L and q_L are coprimes and so is p_R and q_R. This is because any common factor of p_L and q_L must divide the

products $p_L q_R$ and $p_R q_L$ and hence the difference $p_L q_R - p_R q_L = \pm 1$. Any two fractions satisfying Eq. (3) are two neighboring fractions in the Farey tree and are known as the *friendly fractions*. The Farey tree is constructed by applying the Farey sum rule to $\frac{p_L}{q_L}$ and $\frac{p_R}{q_R}$—the Farey parents that give a new fraction $\frac{p_c}{q_c}$—the Farey child:

$$\frac{p_c}{q_c} = \frac{p_L + q_R}{q_L + q_R}. \qquad (4)$$

Analogous to the friendly pair $\frac{p_L}{q_L}$ and $\frac{p_R}{q_R}$, $\frac{p_c}{q_c}$ also forms a friendly pair with each of its parents $\frac{p_L}{q_L}$ and $\frac{p_R}{q_R}$, satisfying the following two equations:

$$p_L q_c - p_c q_L = \pm 1, \qquad (5)$$

$$p_c q_R - p_R q_c = \pm 1. \qquad (6)$$

This implies that p_c and q_c are also coprime. In other words, the entire Farey tree consists of all fractions $\frac{p}{q}$, where p and q are coprime. These equations define a Farey triplet denoted as $[\frac{p_L}{q_L}, \frac{p_c}{q_c}, \frac{p_R}{q_R}]$, which will be referred to as the *friendly Farey triplet*.

The importance of friendly Farey triplets in the butterfly spectrum was pointed out in our recent studies [2,8,9]. It was shown that the magnetic flux values corresponding to friendly triplets $[\frac{p_L}{q_L}, \frac{p_c}{q_c}, \frac{p_R}{q_R}]$ in the Farey tree form the left boundary,

the center, and the right flux boundaries of the butterflies, encoding the hierarchical structure of the butterfly graph as shown in Fig. 2. In other words, the butterfly graph is an incarnation of the Farey tree adorned with butterflies.

III. RELATING FAREY TREE AND THE WANNIER DIAGRAM

To show that the two hierarchical sets—the Farey tree and the Wannier diagram—are related, we first review an alternate way to construct the Farey tree as described by Hatcher [17]. Figure 3 shows the construction of the Farey tree in stages, as we summarize below.

(1) Start with drawing a unit square and its diagonals.

(2) Draw a vertical line from the intersection point of the diagonals down to the bottom edge of the square. Starting with two rational numbers $\frac{0}{1}$ and $\frac{1}{1}$, it gives a new rational number $\frac{1}{2}$. The process generates two trapezoids: one to the left of $\frac{1}{2}$ with parallel lines at $\frac{0}{1}$ and $\frac{1}{2}$ and another to the right of $\frac{1}{2}$ with parallel lines at $\frac{1}{2}$ and $\frac{1}{1}$.

(3) Repeat the above process with each trapezoid, that is, draw its diagonals and then draw vertical lines to the bottom from the intersection point of the diagonals of the trapezoids. This gives the Farey fractions $\frac{1}{3}$ and $\frac{2}{3}$. The vertical line from each of the fractions generates two new trapezoids, one to the left and the other to the right of that fraction.

(4) Continue this process: With each new trapezoid, draw its diagonals and the vertical line from the point of intersection of the diagonals. This will generate all rationals because the vertical lines from the diagonals of the trapezoid formed by two parallel lines at $\frac{p_L}{q_L}$ and $\frac{p_R}{q_R}$ meet the bottom edge at $\frac{p_L+p_R}{q_L+q_R}$—the Farey sum of the two fractions. This is shown in panel (D).

(5) In general, for every trapezoid so formed with two parallel lines at friendly fractions $\frac{p_L}{q_L}$ and $\frac{p_R}{q_R}$, the y coordinates of the upper left and the upper right corners of the trapezoid are $\frac{1}{q_L}$ and $\frac{1}{q_L}$. The coordinate of the intersection of the diagonals is $(\frac{p_L+p_R}{q_L+q_R}, \frac{1}{q_L+q_R})$. By induction, this proves that the length of every vertical line of the trapezoid at fraction $\frac{p}{q}$ is $\frac{1}{q}$.

From this geometrical construction of the Farey tree, we now show that the Farey tree is closely related to the Wannier diagram, an important result.

As illustrated in the upper panels of Fig. 3, relating the Farey tree to the Wannier diagram involves symmetrization of the Farey construction about the $y = \frac{1}{2}$ line of the square. In other words, as the unit square is transformed into a two-torus, the resulting geometrical figure is the Wannier diagram where the $x - y$-axes are identified as the variables $\phi - \rho$ of the Wannier diagram.

In summary, starting with the geometrical construction of the Farey tree (Fig. 3), the Wannier diagram emerges in two steps. First, all vertical lines are extended up to the upper edge of the unit square, which is identified with the $\rho = 1$ line of the Wannier diagram. Second, new lines are added so the entire configuration is symmetrical about $\rho = 1/2$. In other words, the density ρ as a function of ϕ satisfies the condition $\rho(\phi) = \rho(1 - \phi)$.

TABLE I. The slopes and the y intercepts of the diagonals denoted as $(\sigma_{\pm}, \tau_{\pm})$ and nonparallel lines $(\sigma_{\uparrow,\downarrow}, \tau_{\uparrow,\downarrow})$ of the trapezoidal cells shown in Fig. 3(d1), where $p_L q_R - p_R q_L = \pm 1$.

$\sigma_+, \ \tau_+$	$\pm[n_L q_R - (n_R + 1)q_L], \ \mp[n_L p_R - (n_R + 1)p_L]$
$\sigma_-, \ \tau_-$	$\pm[(n_L + 1)q_R - n_R q_L], \ \mp[(n_L + 1)p_R - n_R p_L]$
$\sigma_\uparrow, \ \tau_\uparrow$	$\pm[(n_L + 1)q_R - (n_R + 1)q_L], \ \mp[(n_L + 1)p_R - (n_R + 1)p_L]$
$\sigma_\downarrow, \ \tau_\downarrow$	$\pm[n_L q_R - n_R q_L], \ \mp[n_L p_R - n_R p_L]$

The key point to be noted is that all the slanting lines in Fig. 3 have integer slopes and integer intercepts when the parallel lines of the trapezoid are at friendly fractions and the height of each parallel line at fraction $\frac{p}{q}$ is $\frac{1}{q}$. To see this, consider a general trapezoid, shown in Fig. 3(d1), for example, the diagonal line with a positive slope, denoted as $\sigma_+ = \pm(\frac{n_R+1}{q_R} - \frac{n_L}{q_L})/(\frac{p_R}{q_R} - \frac{p_L}{q_L}) = (n_R + 1)q_L - n_L q_R$ as $p_L q_R - p_R q_L = \pm 1$. Table I lists slopes and intercepts of all nonparallel lines of the trapezoid.

IV. FAREY-WANNIER LATTICE AND THE BUTTERFLY GRAPH

The Wannier trajectories form a very special type of hierarchical lattice made up of trapezoidal cells in every Farey interval $[\frac{p_L}{q_L} - \frac{p_R}{q_R}]$, where the Farey fractions $\frac{p_L}{q_L}$ and $\frac{p_R}{q_R}$ are neighbors in the Farey tree, i.e., they satisfies the friendly fraction condition $p_L q_R - p_R q_L = \pm 1$. The points of intersections of the diagonals of the trapezoids represent the center of the butterfly. In this lattice, all slanting lines have integer slopes
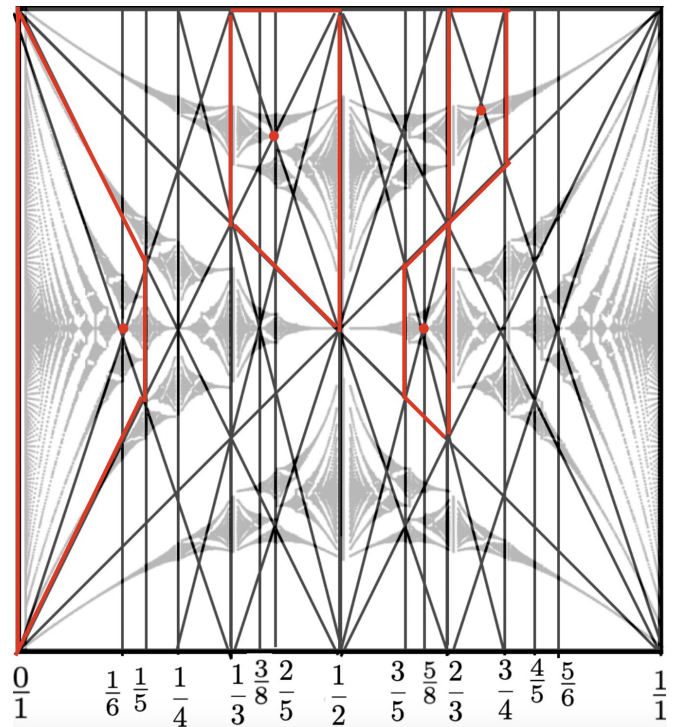

FIG. 4. Butterfly graph with four of its sub-butterflies identified by (red) dots at the center and the corresponding trapezoidal cells (in red) of the Farey-Wannier lattice.
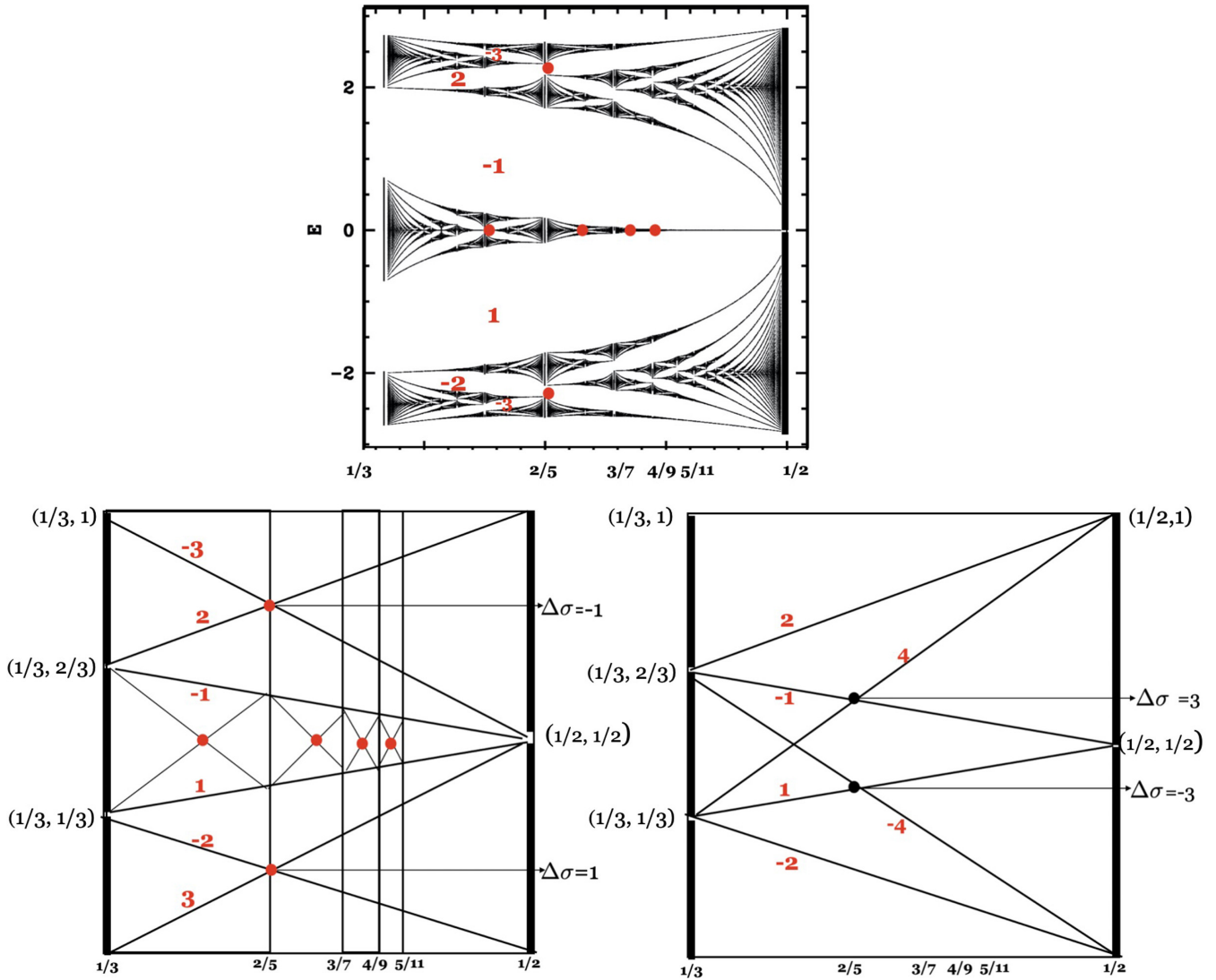
FIG. 5. In the friendly interval $[1/3 - 1/2]$, the upper panel shows a chain of butterflies at the center, a butterfly at the upper edge and a butterfly at the lower edge. Lower left panel shows the corresponding Wannier diagram. The right panel shows another possible Farey-Wannier lattice in this interval. However, such a lattice of trapezoids whose centers are marked with black dots, does not correspond to butterfly configuration. Coordinates of various points and the slopes of various Wannier trajectories (in red) along with the $\Delta\sigma$ corresponding to the trapezoidal cells are shown. Figure illustrates how quantum mechanics *improvises* on the number theory encoded in the Wannier diagram to create butterflies as it chooses only certain trapezoids (shown with red dots) that represent butterflies. The flux interval $[1/3, 1/2]$ supports only two butterflies exhibiting horizontal mirror symmetry about $\rho = \frac{1}{2}$, corresponding to the asymmetry parameter $\Delta\sigma = 1$ and -1, respectively. Wannier trajectories, shown to intersect at black dots correspond to $\Delta\sigma = \pm 3$ and do not correspond to any butterflies. In other words, the butterflies exhibit minimum violation of mirror symmetry.

and also integer intercepts. As described below in Sec. IV B, not all trapezoidal cells correspond to butterflies. Such a hierarchical lattice where every trapezoid represents a butterfly will be dubbed the Farey-Wannier lattice as shown in Fig. 4, where the butterfly graph is superimposed on the Wannier diagram.

A. Nests and chains

Characterization of the Hofstadter butterfly graph consisting of nests and chains as described in our recent study [8] emerges naturally in Farey-Wannier lattice representation of the butterfly graph. In general, a friendly interval $[\frac{p_L}{q_L} - \frac{p_R}{q_R}]$, where ($q_L < q_R$), consists of a stack of q_L trapezoids and

($q_R - q_L$) triangular regimes. With trapezoids representing butterflies, the triangular regimes get partitioned into an infinite chain of trapezoids of different widths that asymptotically approaches zero. In other words, triangular regions of the Farey-Wannier lattice represent a chain of butterflies and each trapezoid is infinitely nested. Figure 5 shows a slab of hierarchical lattice in a friendly interval $[1/2 - 1/3]$ with trapezoids and triangles which overlay the corresponding butterfly graph. This interval consists of two trapezoids representing two butterflies. With higher order Farey fractions, each butterfly gets infinitely nested. This is further illustrated in Fig. 6 with three friendly intervals $[2/7 - 1/3]$, $[1/3 - 2/5]$, $[2/5 - 3/7]$. As described below, not all trapezoids represent butterflies.
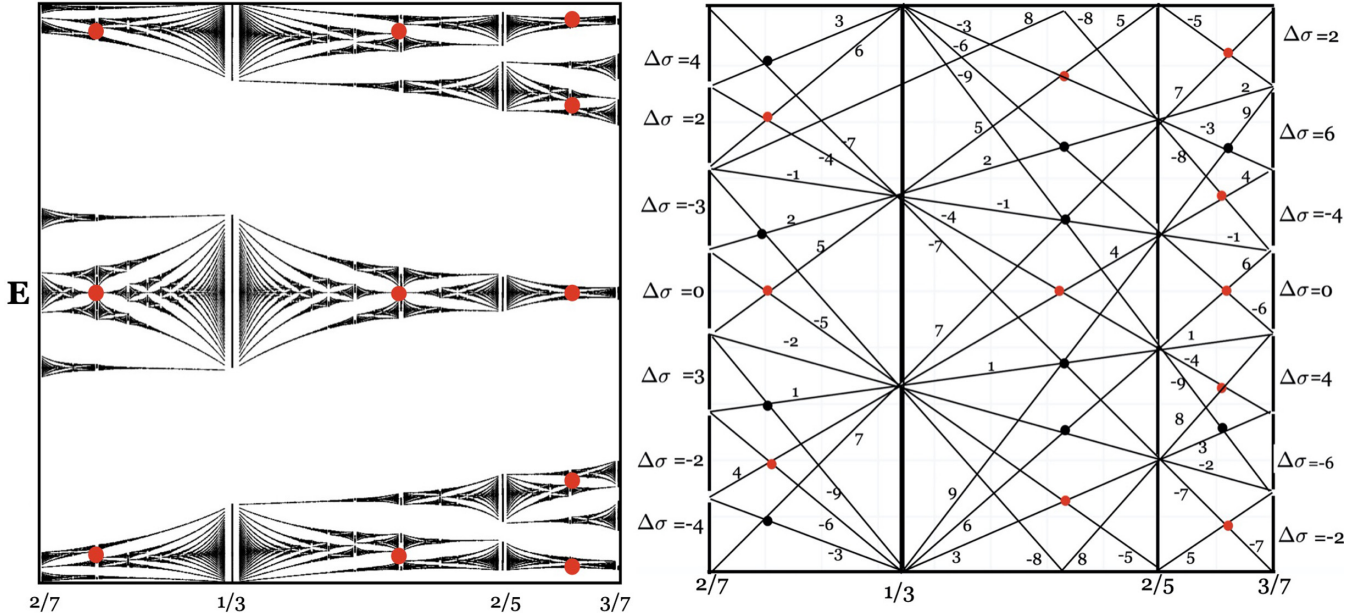
FIG. 6. Butterfly and the corresponding Wannier diagram in three friendly magnetic flux intervals [2/7, 1/3], [1/3, 2/5], and [2/5, 3/7]. Each trapezoid is uniquely determined by a dot (red or black) at the intersection of the two diagonals. Red dots represent the configurations that correspond to the butterflies and can be paired with the red dots in the butterfly graph on the left. Configurations corresponding to black dots do not appear—a feature not determined by the number theoretical arguments. Trapezoids with black dots are forbidden configurations that correspond to higher values of $\Delta\sigma$—the asymmetry parameter, shown explicitly for the left and the right trapezoids. For central interval [1/3, 2/5], the values of $\Delta\sigma = 2, -4, 6, 0, 4, -6$ (from top to bottom). The trapezoids with horizontal mirror symmetry have $\Delta\sigma = 0$.

B. Minimal Symmetry violation

Figures 5, 6, and 8 illustrate an arbitrariness in the choice of selecting trapezoidal and triangular regimes, as we seek one-to-one correspondence between the trapezoids and butterflies. In constructing a Farey-Wannier lattice representing an isomorphism between the hierarchy of trapezoids and butterflies, we now address the key question of what determines the *right* choice of grouping trapezoidal and triangular regimes of the lattice, shown with red dots in the Figs. 5, 6, and 8. The configurations corresponding to black dots are not *used* in the butterfly graph and are rejected. A close inspection of the correspondence between the Farey-Wannier lattice and the butterfly graph shows that the trapezoid cells that do not represent a butterfly can be singled out by a parameter that characterizes the *degree of violation of horizontal mirror symmetry*. Such a symmetry corresponds to the difference in the magnitude of Chern numbers (σ_+, σ_-) as for the central butterflies that exhibit mirror symmetry $|\sigma_+| = |\sigma_-|$. We define a parameter $\Delta\sigma$ as

$$\Delta\sigma = |\sigma_+| - |\sigma_-| = |(2n_R + 1)q_L - (2n_L + 1)q_R|. \quad (7)$$

For central trapezoids, $\Delta\sigma = 0$ as $n_R = \frac{q_R - 1}{2}$, $n_L = \frac{q_L - 1}{2}$. In a given interval $[\frac{p_L}{q_L} - \frac{p_R}{q_R}]$, defined by the friendly fractions, there exists q_L butterflies (when $q_L < q_R$), each characterized by a unique $\Delta\sigma$. Therefore, $\Delta\sigma$ can be taken as a measure of the asymmetry of the trapezoid (and the corresponding butterfly) as the higher the value of $\Delta\sigma$, the greater the degree of violation of horizontal mirror symmetry. The trapezoids that are not paired with butterflies correspond to higher values of $\Delta\sigma$. In other words, given all possible trapezoids in a given rectangular strip, each labeled with a unique value of

$\Delta\sigma$, nature *uses* trapezoids with smallest possible value to represent butterflies in the butterfly graph.

Figures 5, 6, and 8, where all allowed and forbidden configurations are labeled with a unique value of $\Delta\sigma$, provide a rather convincing case of the empirical rule of minimal symmetry violation by the butterflies. Demonstration of the rule in a very narrow flux friendly magnetic flux interval $[7/17 - 12/29]$(also see Fig. 7) is particularly important as the panel IV Fig. 8 shows the allowed and forbidden configurations corresponding to two consecutive allowed values of $\Delta\sigma$ as the allowed values of $\Delta\sigma$ are even integers.

V. NEW SPECIES OF BUTTERFLIES

We now discuss the number theoretical properties of the energy spectrum in a generalized Harper Model [11–14] described by the tight-binding Hamiltonian:

$$H = t_a \cos p + t_b \cos x + t_{ab}[\cos(x - p) + \cos(p - x)]. \quad (8)$$

Here t_a and t_b are NN hopping along the x and y directions and t_{ab} defines the NNN hopping between the diagonals of the square lattice.

As we tune the parameters, the energy spectrum shows changes, although the patterns resembling butterflies persist. We examine the role of number theory in characterizing the energy spectrum with a key question whether the Farey sum rule [Eq. (4)] continues to define the butterflylike spectrum.

In our study of the NNN model spectrum, the Farey hierarchy was found to prevail. However, in addition to butterflies that obey the Farey sum rule, which we refer to as type-I butterflies, there are type-II and type-III butterflies, where the Farey triplet $[\frac{p_L}{q_L}, \frac{p_c}{q_c}, \frac{p_R}{q_R}]$ does not form a friendly triplet. The
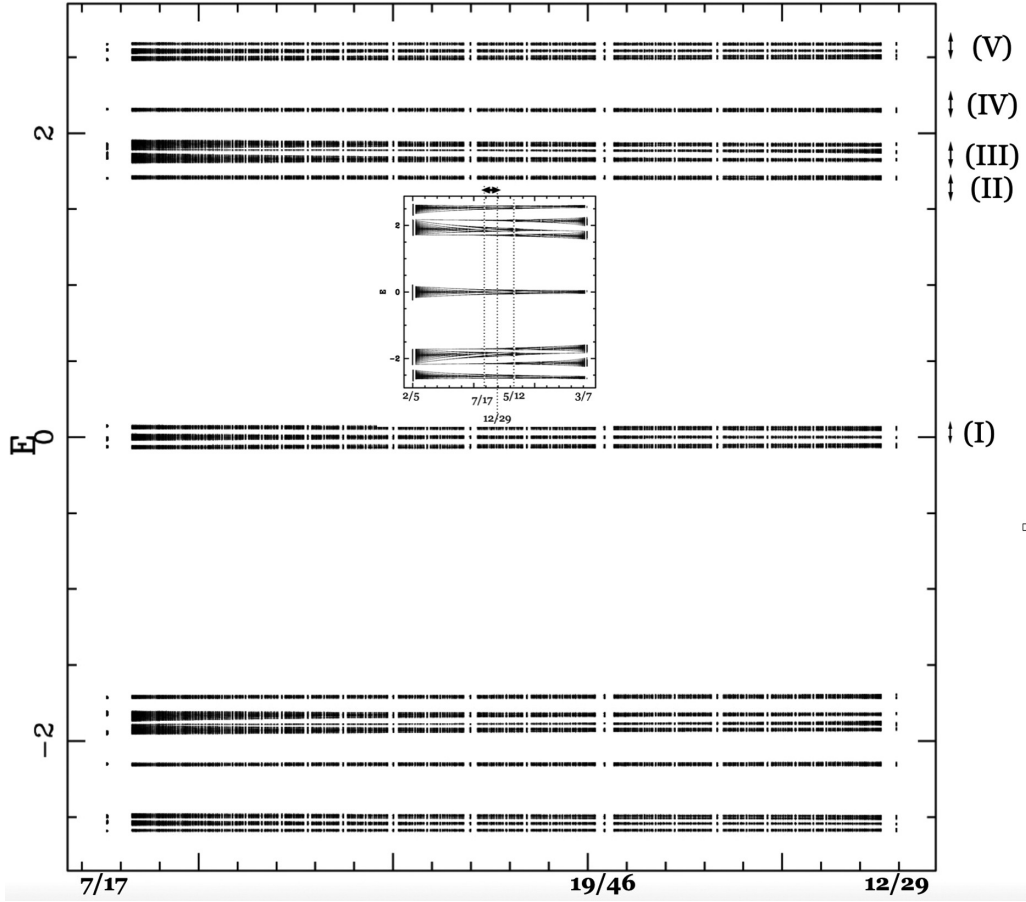
FIG. 7. The butterfly graph in the friendly flux interval [7/17 − 12/29]. An insert at the center (inside the gap) shows the relative location of this narrow flux interval with respect to the flux interval [2/5 − 3/7] that is shown in Fig. 6. Blowups of regions marked on the right (I–V), along with the double arrows are shown in Fig. 8.

modified Farey sum rules for these species of butterflies are given below.

For type-II butterflies:

$$p_L q_R - p_R q_L = \pm 2, \quad p_c q_R - p_R q_c = \pm 1,$$
$$p_c q_L - p_L q_c = \pm 1. \tag{9}$$

Consequently, $p_c = \frac{p_L + p_R}{2}$ and $q_c = \frac{q_L + q_R}{2}$.

For type-III butterflies:

$$p_c q_R - p_R q_c = \pm 2, \quad p_c q_R - p_R q_c = \pm 1,$$
$$p_L q_R - p_R q_L = \pm 1. \tag{10}$$

Therefore, $p_L = \frac{p_c - p_R}{2}$ and $q_L = \frac{q_c - q_R}{2}$

or

$$p_c q_L - p_L q_c = \pm 2, \quad p_c q_L - p_L q_c = \pm 1,$$
$$p_L q_R - p_R q_L = \pm 1, \tag{11}$$

and therefore $p_R = \frac{p_c - p_L}{2}$ and $q_R = \frac{q_c - q_L}{2}$

Therefore, $p_x q_y - p_y q_x = \pm 1$ is true for two of the three pairs from (L, c, R). For the third pair, $p_x q_y - p_y q_x = \pm 2 \equiv D$. That is, among the three pairs of magnetic flux fractions at the left and right boundaries and at the center, two pairs are NN in the Farey tree and one pair is NNN in the tree.

Figure 10 shows an example of the spectrum for special parameter values $t_a = t_{ab} = 1$ and $t_b = 0$, where butterflies

satisfying modified Farey sums (9) and (10) are labeled with green and blue dots, respectively. The blowups of the spectrum, as shown in the right panels, reveal an orderly placement of three species, adding a unique type of order and richness to the butterfly spectrum of the Harper model. Apart from clear differences in their number theoretical properties, characteristic patterns are seen to be associated with each of the three types of butterflies and this helps in visual identification of the new butterflies in the generalized Harper spectrum. Furthermore, the location of the three distinct classes of butterflies appear to be somewhat correlated, indicating a rather mysterious entanglement among the three species.

Distinction between the types I–III, as illustrated in Fig. 9 is further summarized in Table II.

A. Self-similarity for the butterflies

Our previous studies have discussed in detail the self-similar hierarchies of type-I butterflies where the magnetic flux interval for every sub-butterfly is related to the main butterfly by a Möbius transformation [9]. The Appendix provides a broader perspective on the recursions that accommodates the types I–III. Here we give examples illustrating self-similarity of the type-II and type-III butterflies.
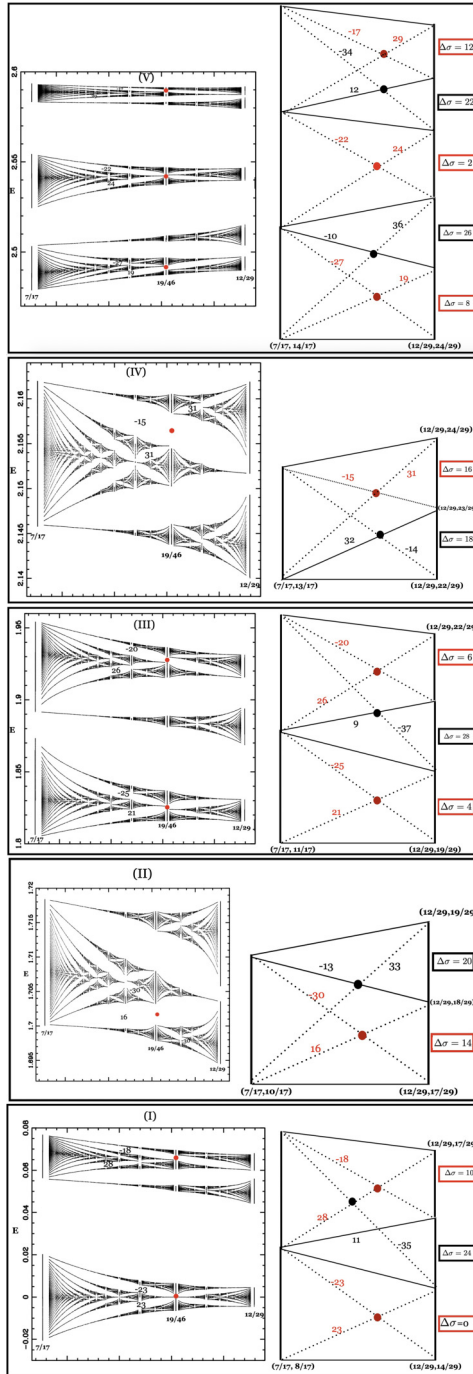
FIG. 8. Blowups of regions (1–5) marked in Fig. 7 corresponding to friendly interval $[7/17 - 12/29]$ and the corresponding Wannier diagrams, illustrating allowed (red dots) and forbidden (black dots) at the points of intersections of the diagonals of the trapezoidal configurations. With 17 vertically stacked butterflies symmetrically placed about $E = 0$ as shown in Fig. 7, this figures show only nine butterflies consisting of the central butterfly and the eight butterflies above the center. The butterflies below the central butterflies are related by symmetry to the butterflies above the center. These nine butterflies are shown in five panels representing the five segments labeled in Fig. 7. The corresponding Wannier diagram on the right displays the allowed and the forbidden configurations, also labeled with the corresponding (color coded) $\Delta\sigma$ values.

Figure 9 shows three levels of recursions for the central band of the spectrum, corresponding to the type-II butterfly triplets $[1/3, 1/4, 1/5] \rightarrow [4/19, 3/14, 2/9] \rightarrow [15/71, 11/52, 7/33]$. The renormalization equation can be constructed by relating the first two levels of the hierarchy, namely, $[1/3, 1/4, 1/5] \rightarrow [4/19, 3/14, 2/9]$. From the level-1 triplet $[1/3, 1/4, 1/5]$, we pick any two fractions and relate it to the corresponding fractions in a level-2 triplet $[4/19, 3/14, 2/9]$, constructing a Möbius map as described in the Appendix. The resulting transformation is independent of the choice of the pair of friendly fractions used to construct the transformation and all three choices give the transformation matrix $T = \begin{bmatrix} -1 & 1 \\ -6 & 5 \end{bmatrix}$ as described in Eq. (A3). The scaling exponent is found to be $2 + \sqrt{3}$, falling in the universality class of the Harper model.

Analogously, Fig. 11 shows the hierarchical structure for a type-III butterfly corresponding to the butterfly triplets $[3/8, 7/18, 2/5] \rightarrow [13/34, 23/60, 5/13] \rightarrow [49/128, 85/222, 18/47]$. The scaling factor is again found to be $\zeta = 2 + \sqrt{3}$.

We conclude with two important remarks about the the transformation T that maps one pair of Farey fractions $(\frac{p_x}{q_x}, \frac{p_y}{q_y})$ to another pair $(\frac{p'_x}{q'_x}, \frac{p'_y}{q'_y})$, preserving the determinant $D = p_x q_y - p_y q_x = p'_x q'_y - p'_y q'_x$ and the order of fractions, namely, $\frac{p_x}{q_x} \rightarrow \frac{p'_x}{q'_x}$ and $\frac{p_y}{q_y} \rightarrow \frac{p'_y}{q'_y}$.

(1) The transformation matrix T in Eq. (A3) describes the recursions for the type-I, type-II, and type-III butterflies. Furthermore, if at least two of the fractions in the Farey triplet $[\frac{p_L}{q_L}, \frac{p_c}{q_c}, \frac{p_R}{q_R}]$ that characterize butterflies are friendly fractions, the determinant D is unity and trace of T is an integer. This implies that the scaling exponent ζ is an irrational number of the form $\zeta = [n^* + 1; \overline{1, n^*}]$ and therefore the scaling associated with all three types of butterflies belongs to the same universality class. However, Eq. (A3) includes the possible scenario where none of the pairs of fractions in the Farey triplet $[\frac{p_L}{q_L}, \frac{p_c}{q_c}, \frac{p_R}{q_R}]$ are friendly fractions and transformation maps two fractions with $D \neq 1$. This will lead to other universality classes, different from the class that describes type-I butterflies. Whether the NNN model described here supports these classes of butterflies has not been seen in our limited exploration of the parameter space.

(2) Missing in these recursions are the renormalizations of $\sigma_\pm$, $(\sigma_\uparrow, \sigma_\downarrow)$, and $\Delta\sigma$. In view of the fact that Wannier trajectories have integer slopes and integer intercepts suggests that the required recursions may mimic the simplicity and the elegance found in the Farey tree hierarchy. However, these equations have remained elusive so far.

B. Anomalous bands

The energy spectrum of the generalized Harper model hosts type-I, type-II, and type-III butterflies. This raises the natural question: Which bands of the energy spectrum transform from type I to type II or type III and which bands remain unchanged as NNN coupling t_{ab} is tuned. In the Harper model, there are bands with ambiguous Chern numbers as the Chern number to the left and right of the band are not the same,
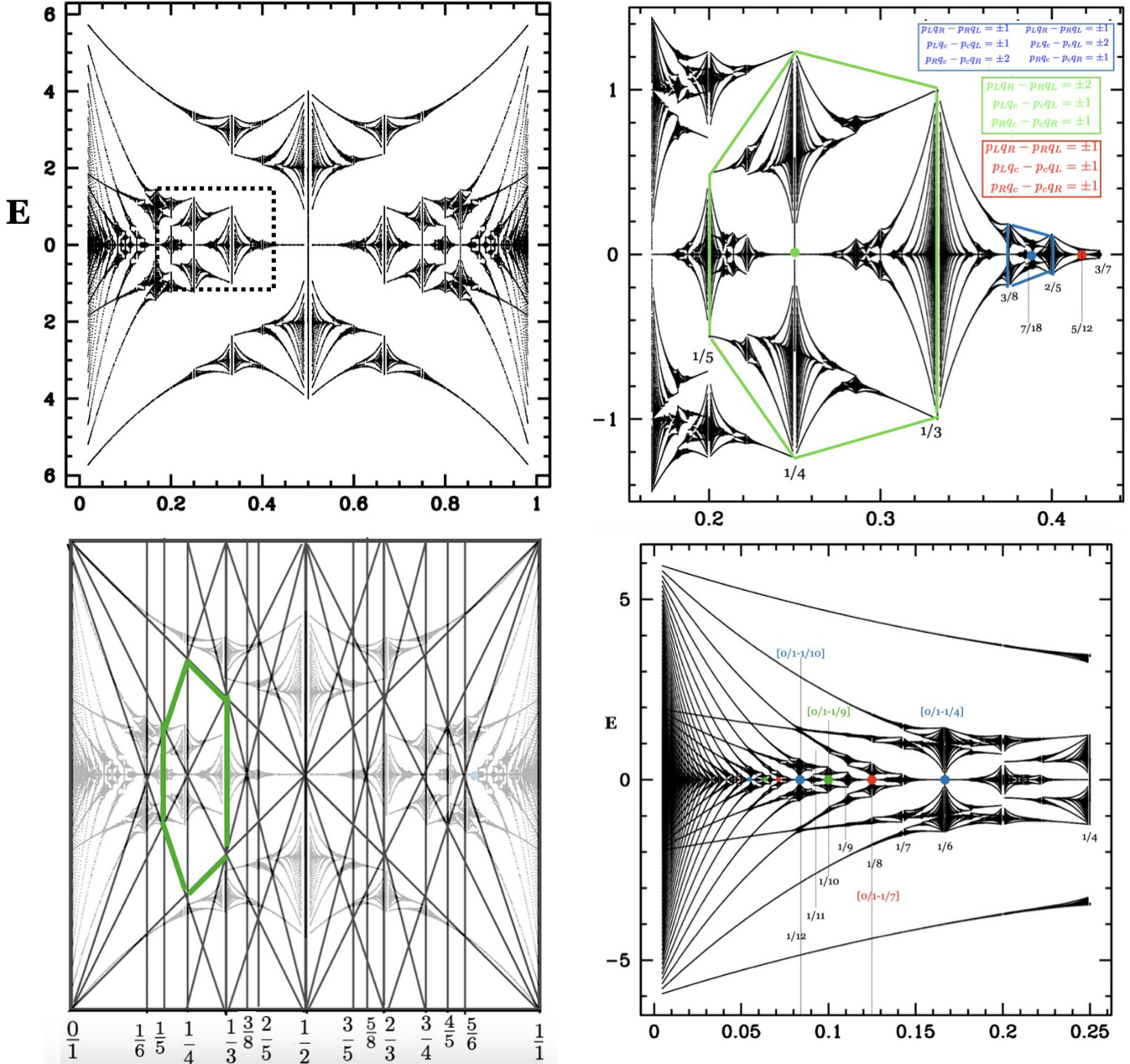
FIG. 9. Upper left panel shows the butterfly graph for $t_{ab} = t_a = 1$ and $t_b = 0$. Lower panel overlays the butterfly graph and the corresponding Wannier diagram showing an example of a hexagonal cell. The right panels show blowups of the upper left panel identifying type-I (red), type-II (green), and type-III (blue) sub-butterflies and the corresponding Farey relations, all color coded. The upper right panel is a zoomed version of the dotted box. Figures 10 and 11 below show the self-similar blowups of the flux intervals $[1/5 - 1/3]$ (type-II, green hexagonal) and $[3/8 - 2/5]$ (type-III, blue trapezoid) shown explicitly in this panel. Lower right panel shows chain of three species of butterflies. For some of the butterflies, the flux intervals $[p_L/q_L - p_R/q_R]$(color coded) shown at the center of the butterflies along with the Farey fractions that define the boundaries and the centers of the butterflies.

as is the case for the central band at $\phi = 1/3$. Two of the butterflies that share this band are $[2/7, 3/10, 1/3](N = 4)$ and $[1/3, 3/8, 2/5(N = -2)$. The two possible values 4 and -2 are two possible solutions of the Diophantine equation $qM + pN = 1$ as it has infinity of solutions $N = N_0 + nq$ as $4 = -2 + 2.3$ with $N_0 = -2$ and $n = 2$. Such bands appear to transform in the presence of NNN terms, transforming the type-I butterfly to to type II.

VI. SUMMARY AND CONCLUSIONS

The Wannier diagram, also known as the gap labeling theory, encodes some of the quintessential features of the energy spectrum of Bloch electrons. Discovered soon after the discovery of the butterfly graph, this alternative elegant description provided an important benchmark for laboratory realization of the butterfly spectrum. In this paper, the Farey tree—a beautiful part of number theory, is shown to to be
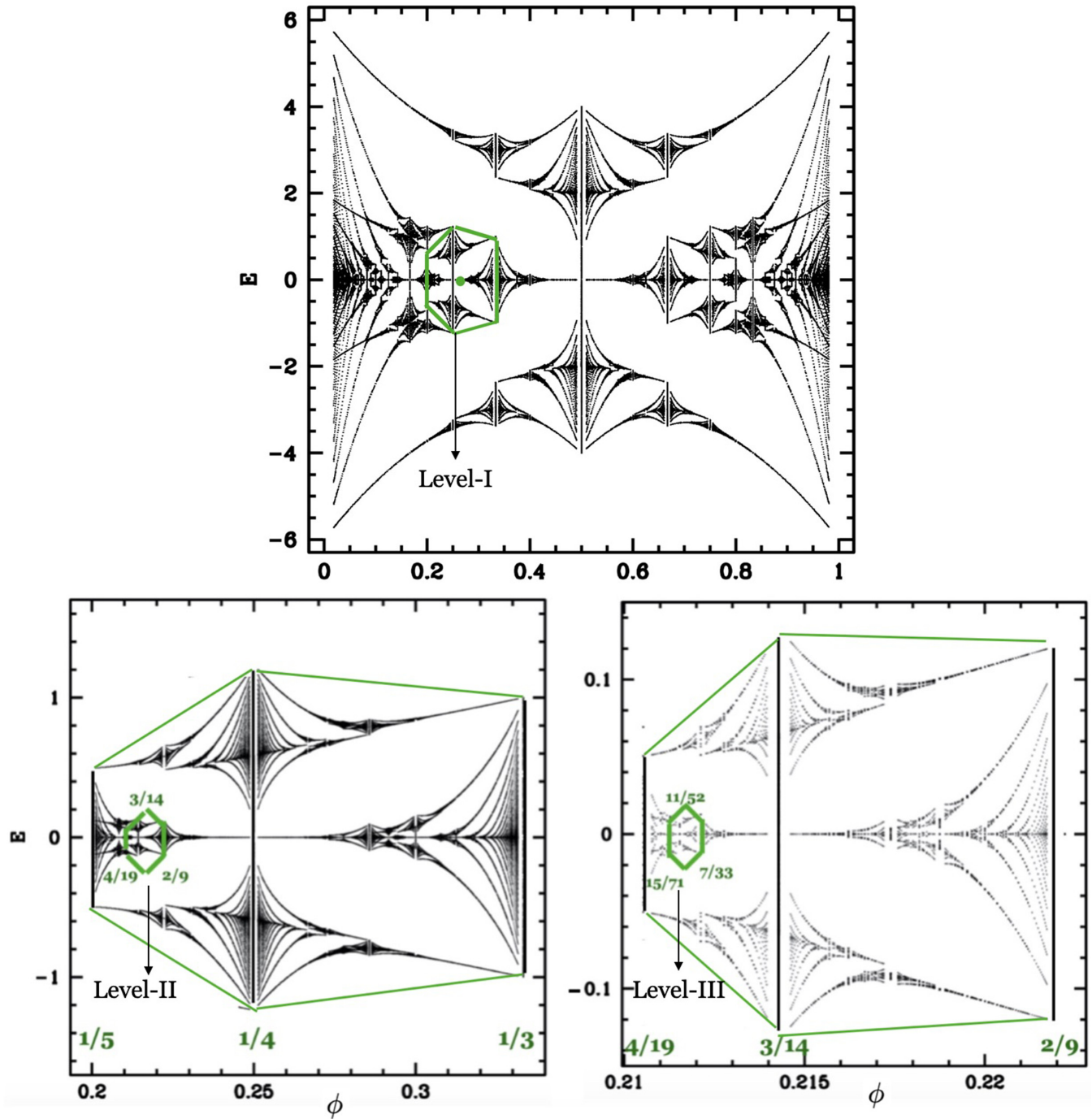
FIG. 10. For parameters corresponding to Fig. 9, the three panels show three levels of blowups of a type-II butterfly (inside green hexagonal). Asymptotically, the blowups approach a self-similar structure.

intimately related to the Wannier diagram. Consequently, the butterfly graph can be viewed as an incarnation of an abstract mathematical set that organizes all rationals between 0 and 1, adding an immense simplicity and mystique to remarkable complexity of Bloch electrons in a magnetic field involving interplay between two competing periodicities. The central to this rather intriguing and nonintuitive simplicity lurking in the butterfly graph is based on the key observation that the process of constructing a Farey tree involves straight lines that have integer slopes and integer intercepts. Alternatively,

submerged in the Wannier diagram—a graph of straight lines with integer slopes and integer intercepts—is a hierarchical lattice of trapezoids whose parallel lines are perpendicular to the x axis, representing two fractions that are neighbors in the Farey tree. Stated more explicitly, given two vertical lines drawn at fractions $\frac{p_L}{q_L}$ and $\frac{p_R}{q_R}$ to the x axis of lengths $\frac{1}{q_L}$ and $\frac{1}{q_R}$, respectively, where $p_L q_R - p_R q_L = \pm 1$, creates trapezoids whose diagonals and slanting lines have integer slopes and integer intercepts. Constructing a hierarchy of this lattice using the Farey sum rule and stacking such trapezoids

TABLE II. Summary of type-I, type-II, and type-III butterflies which are color coded in red, green, and blue in the Fig. 8.

	Type I	Type II	Type III
Farey rule	$\frac{p_c}{q_c} = \frac{p_L+q_R}{q_L+q_R}$	$\frac{p_c}{q_c} = \frac{\frac{p_L+p_R}{2}}{\frac{q_L+q_R}{2}}$,	$\frac{p_L}{q_L} = \frac{\frac{p_c-p_R}{2}}{\frac{q_c-q_R}{2}}$ or $\frac{p_R}{q_R} = \frac{\frac{p_c-p_L}{2}}{\frac{q_c-q_L}{2}}$
(M_x, N_x)	$M_L = M_R, N_L = N_R$	$M_L \neq M_R, N_L \neq N_R$	$M_L = M_R, N_L = N_R$
Representative cell in the Farey-Wannier lattice	Trapezoid	Hexagonal	Trapezoid
Conformally related to main butterfly	Yes	No	No

symmetrically in a unit square generates the entire Wannier diagram.

Dwelling mostly on the number theoretical aspects of the butterfly spectrum, here we also unveil a simple rule that captures a non-number-theoretical characteristic. Our observation that not all Wannier trajectories find representation in the butterfly graph can be stated as a simple rule of minimal violation of symmetry of the butterflies. In other words, quantum mechanics of Bloch electrons in a magnetic field improvises on number theory to generate the butterfly spectrum. We hope that this empirical result based on very extensive numerical studies can be proven rigorously using renormalization theory.

In a generalized Harper model, the Farey hierarchy prevails. Intriguingly, the NNN model uses NNN Farey fractions to create unique species of butterflies. These butterflies with somewhat different number theoretical characteristics are not the exact replica of the main butterfly. However, their recursions can be described by the renormalization group framework that describes the recursive structure of the Harper model. What perturbations take us outside this renormalization and perhaps outside the number theoretical description inherent in the energy spectrum remains an interesting open question.

Our brief discussion of the butterfly graph in the NNN model explores a very small part of the multidimensional parameter space of the NNN model. Furthermore, However, this preliminary number theoretical and numerical studies of the generalized Harper model show immense richness, order, and complexity, indicating a very fertile and new field of research in the subject of Bloch electrons in a magnetic field. Although these species of butterflies were found to be described by the universality class of type-I butterflies, that is, are characterized by scaling exponent $\zeta = [1 + n^*; \overline{1, n^*}]$, we point out that the

renormalization equations as described in the Appendix leave open the possibility of new university classes. Furthermore, unlike the Hofstadter butterfly spectrum, other types of butterflies are not replicas of the main butterfly and thus require a type of renormalization different from the Wilkinson renormalization [18,19] that explains the hierarchical structure of the Harper model. Finally, the chain of butterflies consisting of three species as shown in Fig. 9 suggests that the three species of butterflies are somewhat entangled. We hope our studies will stimulate further research in this fascinating field.

APPENDIX: FAREY TREE HIERARCHY AND MÖBIUS TRANSFORMATION

We describe an important symmetry property of the Farey tree where, by the word symmetry, we do not refer to the Euclidean geometrical symmetry, but symmetry described by invertible algebraic transformations that maps one pair of Farey fractions to another. That is, we seek a transformation T,

$$\left(\frac{p_x(1)}{q_x(1)}, \frac{p_y(1)}{q_y(1)}\right) \rightarrow \left(\frac{p_x(2)}{q_x(2)}, \frac{p_y(2)}{q_y(2)}\right) = T\left(\frac{p_x(1)}{q_x(1)}, \frac{p_y(1)}{q_y(1)}\right),$$

(A1)

where each pair satisfies $(p_x(l)q_y(l) - p_y(l)q_x(l)) = D \neq 0$ $(l = 1, 2)$ and the mapping preserves the order, that is, $\frac{p_x(1)}{q_x(1)} \rightarrow \frac{p_x(2)}{q_x(2)}$ and $\frac{p_y(1)}{q_y(1)} \rightarrow \frac{p_y(2)}{q_y(2)}$. To obtain T, we construct two matrices T_1 and T_2 as

$$T_1 = \begin{bmatrix} p_x(1) & p_y(1) \\ q_x(1) & q_y(1) \end{bmatrix}, \quad T_2 = \begin{bmatrix} p_x(2) & p_y(2) \\ q_x(2) & q_y(2) \end{bmatrix}. \quad (A2)$$

We will now show that the required map is [17]

$$T = T_2 T_1^{-1} = \frac{1}{D} \begin{bmatrix} p_x(2)q_y(1) - p_y(2)q_x(1) & p_x(1)p_y(2) - p_x(2)p_y(1) \\ q_x(2)q_y(1) - q_x(1)q_y(2) & p_x(1)q_y(2) - p_y(1)q_x(2) \end{bmatrix}. \quad (A3)$$

To prove Eq. (A3), consider a transformation that maps a primitive fraction $\frac{p}{q}$ to another primitive fraction $\frac{p'}{q'}$, defined as

$$\frac{p}{q} \rightarrow \frac{p'}{q'} = \frac{ap+bq}{cp+dq} \equiv \frac{a\frac{p}{q}+b}{c\frac{p}{q}+d}. \quad (A4)$$

The above equation can also be written as

$$\begin{pmatrix} p \\ q \end{pmatrix} \rightarrow \begin{pmatrix} p' \\ q' \end{pmatrix} = \begin{pmatrix} a & b \\ c & d \end{pmatrix} \begin{pmatrix} p \\ q \end{pmatrix} \equiv \mathcal{M} \begin{pmatrix} p \\ q \end{pmatrix}. \quad (A5)$$

Under this transformation, $\frac{0}{1} \rightarrow \frac{b}{d}$ and $\frac{1}{0} \rightarrow \frac{a}{c}$. In other words, $\mathcal{M}^{-1}$ maps a pair of fractions $(\frac{b}{d}, \frac{a}{c})$ to $(\frac{0}{1}, \frac{1}{1})$.
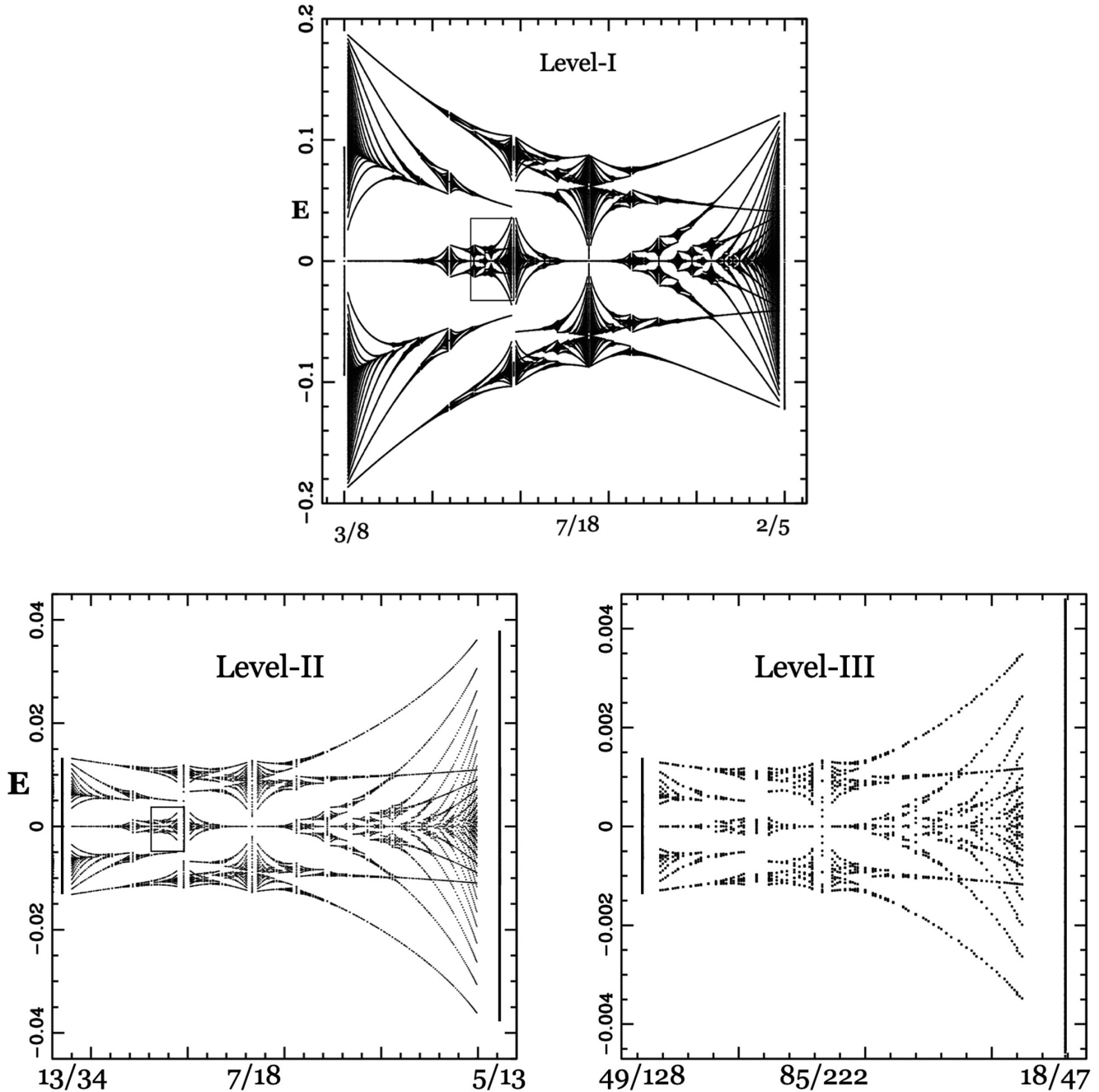
FIG. 11. The three panels shows three levels of blowups of a type-III butterfly shown in the flux interval $[3/8 - 2/5]$ in Fig. 9. Asymptotically scaling exponent corresponds to $\zeta = 2 + \sqrt{3}$.

Therefore, the transformation that maps $(\frac{p_x(1)}{q_x(1)}, \frac{p_y(1)}{q_y(1)})$ to $(\frac{p_x(2)}{q_x(2)}, \frac{p_y(2)}{q_y(2)})$ can be constructed as a two-step process where we first map $(\frac{p_x(1)}{q_x(1)}, \frac{p_y(1)}{q_y(1)})$ to $(\frac{0}{1}, \frac{1}{1})$, where $\begin{pmatrix} a & b \\ c & d \end{pmatrix} = T_1^{-1}$, and then map $(\frac{0}{1}, \frac{1}{1})$ to $(\frac{p_x(2)}{q_x(2)}, \frac{p_y(2)}{q_y(2)})$, where $\begin{pmatrix} a & b \\ c & d \end{pmatrix} = T_2$.

This completes the proof that $T = T_2 T_1^{-1}$ where (T_1, T_2) are given by Eq. (A2).

For self-similar hierarchical structures, the renormalization equation connecting two consecutive levels l and $l + 1$ is

given by

$$\begin{pmatrix} p(l+1) \\ q(l+1) \end{pmatrix} = T \begin{pmatrix} p(l) \\ q(l) \end{pmatrix}. \tag{A6}$$

This equation encoding the Farey tree hierarchy also describes the recursive structure of type-I, type-II, and type-III butterflies. The eigenvalues of T determine the asymptotic scalings of the butterfly flux interval. These eigenvalues are of the form (ζ, ζ^{-1}). This is because the matrix T has real trace and its determinant is unity as from the product rule of the determinant, $\text{Det}[T] = \text{Det}[T_2].\text{Det}[T_1^{-1}] = D.\frac{1}{D} = 1$.

For type-I butterflies, every sub-butterfly is a renormalization of the main butterfly [8,18]. In this recursive scheme, every friendly triplet $[\frac{p_L}{q_L}, \frac{p_c}{q_c}, \frac{p_R}{q_R}]$ is related to $[\frac{0}{1}, \frac{1}{2}, \frac{1}{1}]$ by a conformal map—a Möbius transformation. This transformation can be constructed by choosing a pair of friendly fractions. For example, we can choose $\frac{p_x(1)}{q_x(1)} = \frac{0}{1}$ and $\frac{p_y(1)}{q_y(1)} = \frac{1}{1}$ and we write $\frac{p_x(2)}{q_x(2)} = \frac{p_L^*}{q_L^*}$ and $\frac{p_R(2)}{q_R(2)} = \frac{p_R^*}{q_R^*}$ and obtain a simplified recursion [8,9]:

$$\phi(l+1) = \frac{(p_R^* - p_L^*)\phi(l) + p_L^*}{(q_R^* - q_L^*)\phi(l) + q_L^*} \equiv \begin{bmatrix} (p_R^* - p_L^*) & p_L^* \\ (q_R^* - q_L^*) & q_L^* \end{bmatrix} \begin{bmatrix} p(l) \\ q(l) \end{bmatrix}. \tag{A7}$$

The transformation also maps $\frac{1}{2}$ to ϕ_c as with $\phi(l) = \frac{1}{2}$, we get $\phi(l+1) = \frac{p_L^* + p_R^*}{q_L^* + q_R^*}$

The eigenvalues of the transformation matrix, denoted as (ζ, ζ^{-1}), determine the asymptotic scaling factors and are given by

$$\zeta = \lim_{l \to \infty} \frac{p_x(l+1)}{p_x(l)} = \lim_{l \to \infty} \frac{q_x(l+1)}{q_x(l)} = \frac{(q_L^* + p_R^* - p_L^*)}{2} \pm \sqrt{\left(\frac{q_L^* + p_R^* - p_L^*}{2}\right)^2 - 1}. \tag{A8}$$

Expressed as a continued fraction expansion, these quadratic irrationals are given by

$$\zeta = [n^*+1; \overline{1, n^*}], \quad n^* = q_L^* + p_R^* - p_L^* - 2, \tag{A9}$$

where

$$[n^*+1; \overline{1, n^*}] \equiv n^* + 1 + \cfrac{1}{1 + \cfrac{1}{n^* + \cfrac{1}{1 + \cfrac{1}{n^* + \cfrac{1}{1 + \cfrac{1}{n^* \dots}}}}}} \tag{A10}$$

The scaling exponent (A10) describes type-I, type-II, and type-III butterflies. The possibility of a new universality class requires $|p_x q_y - p_y q_x| = D > 1$ for all three pairs of fractions in a given Farey triplet that defines a butterfly.

[1] D. R. Hofstadter, Phys. Rev. B **14**, 2239 (1976).

[2] I. I. Satija, *Butterfly in the Quantum World* (IOP Concise, Morgan and Claypool, San Raffael, CA, 2016).

[3] V. Galitski, G. Juzeliunas and I. B. Spielman, Phys. Today **72**, 38 (2019).

[4] A. Avila and S. Jitomirskaya, Ann. Math. **170**, 303 (2009).

[5] C. R. Dean, L. Wang, P. Maher, C. Forsythe, F. Ghahari, Y. Gao, J. Katoch, M. Ishigami, P. Moon, M. Koshino, T. Taniguchi, K. Watanabe, K. L. Shepard, J. Hone, and P. Kim, Nature (London) **497**, 598 (2013).

[6] D. J. Thouless, M. Kohmoto, M. P. Nightingale, and M. den Nijs, Phys. Rev. Lett. **49**, 405 (1982).

[7] I. I. Satija, Eur. Phys. J.: Spec. Top. **225**, 2533 (2016).

[8] I. Satija and M. Wilkinson, J. Phys. A **53**, 085703 (2020).

[9] I. Satija, J. Phys. A **54**, 025701 (2021).

[10] P. G. Harper, Proc. Phys. Soc. A **68**, 874 (1955).

[11] F. Claro, Phys. Status Solidi (B) **104**, K31 (1981).

[12] D. J. Thouless, Phys. Rev. B **28**, 4272 (1983).

[13] Y. Hatsugai and M. Kohmoto, Phys. Rev. B **42**, 8282 (1990).

[14] J. H. Han, D. J. Thouless, H. Hiramoto, and M. Kohmoto, Phys. Rev. B **50**, 11365 (1994).

[15] A. Avila, S. Jitomirskaya, and C. A. Marx, Invent. Math **210**, 283 (2017).

[16] I. E. Powell and S. Chakravarty, Phys. Rev. B **100**, 075150 (2019).

[17] A. Hatcher, *Topology of Numbers* (2018).

[18] M. Wilkinson, J. Phys. A: Math. Gen. **20**, 4337 (1987).

[19] M. Wilkinson, Proc. Roy. Soc. A **391**, 305 (1984).

[20] B. Simon, Adv. Appl. Math. **3**, 463 (1982).

[21] G. H. Wannier, Phys. Status Solidi B **88**, 757 (1978).

[22] F. H. Claro and G. H. Wannier, Phys. Rev. B **19**, 6068 (1979).

[23] R. Johnson and J. Moser, Commun. Math. Phys. **84**, 403 (1982); **90**, 317 (1983).

[24] F. Delyon and B. Souillard, Commun. Math. Phys. **89**, 415 (1983).

[25] A. H. MacDonald, Phys. Rev. B **28**, 6713 (1983); **29**, 3057 (1984).

[26] I. Danna, Y. Avron, and J. Zak, J. Phys. C **18**, L679 (1985).